Science of the Total Environment 691 (2019) 1144–1154

Contents lists available at ScienceDirect

Science of the Total Environment

journal homepage: www.elsevier.com/locate/scitotenv

Cyanobacteria in eutrophic waters benefit from rising atmospheric CO_2 concentrations

Jingjie Ma [a,b], Peifang Wang [a,b,*], Xun Wang [a,b], Yi Xu [a,b], Hans W. Paerl [c]

[a] Key Laboratory of Integrated Regulation and Resources Development on Shallow Lakes, Ministry of Education, Hohai University, Nanjing 210098, People's Republic of China
[b] College of Environment, Hohai University, Nanjing 210098, People's Republic of China
[c] Institute of Marine Sciences, University of North Carolina at Chapel Hill, Morehead City, NC 28557, United States

HIGHLIGHTS

- Elevated CO_2 improved photosystem II particularly under nutrient-rich conditions.
- Effects of elevated CO_2 on the EPS of *M. aeruginosa* were related to nutrient level.
- Intracellular acidification may be facilitated in high-CO_2, nutrient-poor waters.
- The AP activity of *M. aeruginosa* improved with higher CO_2 at low nutrient levels.
- Elevated CO_2 inhibited NR activity in *M. aeruginosa* regardless of nutrient levels.

GRAPHICAL ABSTRACT

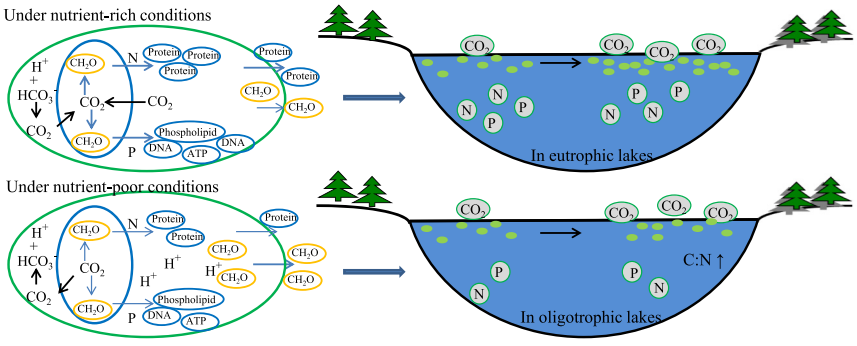

ARTICLE INFO

Article history:
Received 24 April 2019
Received in revised form 3 July 2019
Accepted 4 July 2019
Available online 04 July 2019

Editor: Ouyang Wei

Keywords:
Microcystis aeruginosa
CO_2
Nutrient
Photosynthesis
Extracellular polymeric substance
Acidification

ABSTRACT

Rising atmospheric carbon dioxide (CO_2) may stimulate the proliferation of cyanobacteria. To investigate the possible physiological responses of cyanobacteria to elevated CO_2 at different nutrient levels, *Microcystis aeruginosa* were exposed to different concentrations of CO_2 (400, 1100, and 2200 ppm) under two nutrient regimes (i.e., in nutrient-rich and nutrient-poor media). The results indicated that *M. aeruginosa* differed in its responses to elevated atmospheric CO_2 at different nutrient levels. The light utilization efficiency and photoprotection of photosystem II were improved by elevated CO_2, particularly when cells were supplied with abundant nutrients. In nutrient-poor media, both total organic carbon and the polysaccharide/protein ratio of the extracellular polymeric substance increased with elevated CO_2, accompanied by high cellular carbon/nitrogen ratios. Besides, cells growing with fewer nutrients were more prone to suffer intracellular acidification with elevated CO_2 than those growing with abundant nutrients. Nonetheless, alkaline phosphate activity of cyanobacteria was improved by high CO_2, provided that reduced pH was in the optimum range for alkaline phosphate activity. Nitrate reductase activity was inhibited by elevated CO_2 regardless of nutrient levels, leading to a reduced nitrate uptake. These changes indicate that the biogeochemical cycling of nutrients would be affected by higher atmospheric CO_2 conditions. Overall, cyanobacteria in eutrophic waters may benefit more than in oligotrophic waters from rising atmospheric CO_2 concentrations, and evaluations of the influence of rising atmospheric CO_2 on algae should account for the nutrient level of the ecosystem.

* Corresponding author at: College of Environment, Hohai University, 1 Road Xikang, Nanjing 210098, People's Republic of China.
E-mail address: pfwang2005@hhu.edu.cn (P. Wang).

https://doi.org/10.1016/j.scitotenv.2019.07.056
0048-9697/

1. Introduction

It is well established that anthropogenic activities are dramatically changing the global environment (Boyd and Hutchins, 2012; Brennan and Collins, 2015). Since the industrial age, atmospheric level of carbon dioxide (CO_2) has increased by 40% (Hasler et al., 2016).The trend is likely to persist, potentially increase to ~1000 ppm by the year 2100 from the current level of ~400 ppm (Jansen et al., 2007). As CO_2 rises, both the function and the organismal behavior of aquatic ecosystems may be changed (Hasler et al., 2016). Studies into the impacts of rising atmospheric CO_2 on aquatic ecosystems have largely focused on the marine environment, which is universally recognized as an important sink for atmospheric CO_2 (Hasler et al., 2016). Diatoms alter their growth rates, depending upon the taxon (Mccarthy et al., 2012; Shi et al., 2015), calcifying marine organisms are likely to reduce their calcification capabilities (Lorenzo et al., 2018), and marine fishes may lose their sensitive olfactory responses (Munday et al., 2014) in response to higher levels of CO_2. In contrast, less knowledge have been reported on the potential consequences of elevated atmospheric CO_2 on freshwater ecosystems, even though they are more poorly buffered to pH changes (Hasler et al., 2016).

Freshwater ecosystems are usually thought to be CO_2-supersaturated (Cole et al., 1994). A bulk of carbon (C) in lakes originates from terrestrial primary production, the mineralization of which causes CO_2 to exist at high levels (Hasler et al., 2016). However, the extensive growth of phytoplankton can easily deplete CO_2 within a few hours because they are poorly buffered (Maberly, 2010). Accordingly, an increase in atmospheric CO_2 levels may provide sufficient influx of CO_2 to alleviate C-limitation and enable a substantial increase in the productivity of aquatic primary productivity (Low-Decarie et al., 2015; Visser et al., 2016).

Cyanobacterial blooms in freshwater ecosystems have occurred with increasing frequency and intensity, severely impairing water qualities, drinking, water supplies, irrigation, and fishing. Some existing models and laboratory experiments have shown that rising CO_2 concentrations may exacerbate cyanobacterial blooms (Verspagen et al., 2014a,b). Additionally, it could lead to a reversal in the competitive dominance among toxic and nontoxic *Microcystis* strains (Van de Waal et al., 2011). Cyanobacteria can use CO_2 and bicarbonate for carbon fixation via the ribulose-1,5-bisphosphate carboxylase/oxygenase (RubisCO). To overcome the low affinity of Rubisco for CO_2, cyanobacteria and most other phytoplankton have evolved a CO_2 concentrating mechanism (CCM) (Visser et al., 2016). Cyanobacterial CCM is based on the carbon uptake systems, which transport CO_2 and bicarbonate into cytoplasm. Five different inorganic carbon uptake systems have been identified in cyanobacteria thus far: NDH-I3 and NDH-I4 for CO_2, and BicA, SbtA, and BCT1 for bicarbonate (Price, 2011; Sandrini et al., 2014). These uptake systems have different properties. BicA has a low affinity for bicarbonate but high flux rate. Conversely, SbtA has a high affinity for bicarbonate but low flux rate (Price, 2011). A prior study reported that cyanobacteria with BicA but without SbtA perform well under high CO_2 conditions (Sandrini et al., 2014).

However, CCMs are energy-demanding (Lorenzo et al., 2018). In some phytoplankton, the downregulation of CCM under elevated CO_2 conditions occurs concurrent with rearrangements in metabolic pathways and physiology (Hennon et al., 2017; Rokitta et al., 2012). However, these rearrangements in response to rising CO_2 may depend on the nutrient status. For instance, previous study has reported that not only nitrogen but also carbon metabolism is key to microcystin production (Beversdorf et al., 2015). Microcystin consists of seven amino acids, of which two amino acid positions are variable, resulting in the production of many microcystin variants. These microcystin variants differ not only in their C/N stoichiometry but also their toxicity. Elevated CO_2 has been reported to cause a shift toward more toxic microcystin variants (microcystin-LY) in nitrogen (N)-limited *M. aeruginosa* (Liu et al., 2016), but yield larger amount of less toxic microcystin variants (microcystin-RR) in N-excess *M. aeruginosa* (Van de Waal et al., 2009). Moreover, the diatom *Thalassiosira pseudonana* can increase its photosynthesis and dark respiration rate under the elevated CO_2 (Yang and Gao, 2012). The reverse of these observations have been made under nitrate-limited conditions (Hennon et al., 2014).

Excess nutrient input to freshwater systems has received great attention, as it frequently leads to intense algal blooms (Paerl, 1988; O'Neil et al., 2012). Nitrogen and phosphorus (P) are essential for supporting the synthesis of proteins, nucleic acid, and adenosine triphosphate (ATP) in algae. Therefore, increased N and P availability is expected to affect carbon fixation, photosynthesis and other physiological processes (Conley et al., 2009; Hipkin et al., 1983). Additionally, excessive nutrient input may stimulate C limitation in freshwater (Verspagen et al., 2014a). C availability could also influence nutrient assimilation. It has been reported that *T. pseudonana* reduced its nitrate uptake and nitrate reductase (NR) activity under elevated CO_2 conditions (Shi et al., 2015), while the NR activity of *Emiliania huxleyi* increased linearly with CO_2 (Rouco et al., 2013). These findings suggest that nutrient utilization and carbon metabolism may be tightly coupled. Previous studies have been focused on how the availability of C and nutrients affects ecological stoichiometry. It has been shown that stoichiometric ratios vary over a wide range with elevated CO_2 among species: an increase in *T. pseudonana* (Reinfelder, 2012), a decrease in *Chaetoceros affinis* (Hennon et al., 2017), and a stable ratio of C/nutrients in *Prorocentrum minimum* (Hennon et al., 2017).

Although laboratory experiments have shown that rising CO_2 is likely to increase cyanobacterial biomass, there is little knowledge regarding the possible underlying physiological responses. Moreover, whether or not these responses vary with the amount of nutrients concentrations remains unknown. To fill this knowledge gap, the freshwater cyanobacteria *M. aeruginosa*, a widespread bloom-forming species, was cultured under different CO_2 (400, 1100, and 2200 ppm) and nutrient levels (nutrient-rich and nutrient-poor). The physiological responses to different treatments, including photosynthesis, cell composition, and some enzyme activities, were evaluated for *M. aeruginosa* to determine the influence of elevated atmospheric CO_2 in freshwater environments.

2. Materials and methods

2.1. Experimental setup

The cyanobacterial strain *M. aeruginosa* FACHB-927 was obtained from the Freshwater Algae Culture Collection of the Institute of Hydrobiology (FACHB), Wuhan, Hubei Province, China. Experiments with *M. aeruginosa* were conducted under nutrient-rich and nutrient-poor conditions. *Microcystis aeruginosa* was grown in a Bold 3 N medium, in which the concentrations of nitrate and phosphate were adjusted. Following the methods of Verspagen et al. (2014a), nutrient-rich conditions were induced using high-nitrate (45 mg/L NO_3^-) and high-phosphate (2.5 mg/L PO_4^{3-}) concentrations, allowing for C-limited growth. Nutrient-poor conditions were induced by using low-nitrogen (6 mg/L NO_3^-) and low-phosphate (0.3 mg/L PO_4^{3-}) concentrations, allowing for nutrient-limited growth. These two nutrient regimes were combined with three different CO_2 partial pressures. Six different treatments in this study were abbreviated as: RL, nutrient-rich conditions with 400 ppm CO_2; RM, nutrient-rich conditions with 1100 ppm CO_2; RH, nutrient-rich conditions with 2200 ppm CO_2; PL, nutrient-poor conditions with 400 ppm CO_2; PM, nutrient-poor conditions with 1100 ppm CO_2; PH, nutrient-poor condition with 2200 ppm CO_2. Every treatment was in triplicate. To simulate atmospheric CO_2 supply to water, gas mixtures with 400 ppm CO_2, 1100 ppm CO_2 or 2200 ppm CO_2 were dispersed from the bottom of flasks as fine bubbles at a constant gas flow rate of 2.4 L/h; aeration lasted for 1 h at 9:00, 13:00, and 17:00 every day. At the end of each aeration, the flasks were sealed with Parafilm to minimize gas diffusion. Dissolved CO_2

concentration in the medium was not expected to match CO_2 concentration of gas mixture. The focus was on increased C influx from rising atmospheric CO_2 level. The current atmospheric level was represented as 400 ppm, and 1100 ppm represented the atmospheric level projected for by the end of the 21st century, while 2200 ppm represented a CO_2-stressed level. Cells were inoculated at an initial density of 10^6 cell/mL in 500 mL flasks and then cultivated for 21 days. These flasks were incubated in an illuminated incubator, with lamp (Philips TCH086 TL5-21W) evenly distributed around. The incubator was set at a temperature of 25 °C, an illuminance of 2000 lx, and a light: dark cycle of 12:12 h. The flasks were shaken three times a day to make cells evenly distributed in the medium.

2.2. Measurements

2.2.1. Medium chemistry and cell density

Nitrate concentrations in the media were determined by sampling 2 mL of culture suspension, which was immediately filtered through 0.45-μm membrane filters (Whatman Inc., UK). Nitrate was measured colourimetrically by an AA3 Auto-Analyzer (Seal, Norderstedt, Germany), and pH values were measured with a pH meter (Mettler Toledo, USA). Total alkalinity (TA) was determined in a 3-mL sample that was titrated with 10 mM of HCl to a pH of 3.0. Concentrations of dissolved CO_2, bicarbonate, and carbonate were calculated from TA and CO_2 partial pressures, using the CO2SYS macro (Lewis and Wallace, 1998). Cell density was determined by combining cells count (CytoFLEX, Beckman, Germany) and spectrophotometric reading with 680 nm (TU-1901, Puxi, China).

2.2.2. Photosynthesis and respiration

The quantum yields and non-photochemical quenching (NPQ) of PSII were measured using a Phyto-PAM-II (Hein Walz, Germany) in this study. The quantum yields of energy conversion in PSII were calculated according to the method of Kramer et al. (2004), which can be transformed into the following equations:

$$F_v/F_m = (F_m - F_o)/F_m; \quad (1)$$

$$\mathrm{Y(II)} = (F'_m - F)/F'_m; \quad (2)$$

$$\mathrm{Y(NPQ)} = F/F'_m - F/F_m \quad (3)$$

$$\mathrm{Y(NO)} = F/F_m, \quad (4)$$

where F_m and F_o are the maximum and minimum fluorescence after dark-adaptation, respectively; F corresponds to the momentary fluorescence, and F'_m corresponds to the maximum fluorescence. Finally, Y(II) is the effective photochemical quantum yield, F_v/F_m corresponds to the maximum Y(II), Y(NPQ) is the quantum yield of the light-induced for PSII, and Y(NO) is the quantum yield of non-regulated heat dissipation and fluorescence emissions of PSII. Dark respiration rates were determined with a Clark-type oxygen electrode based on changes in the oxygen concentration over time at 25 °C.

2.2.3. Elemental composition

When cultivation was complete, cellular carbon (POC), nitrogen (PON), and particulate organic P (POP) were measured. The POC and PON were analyzed using a Vario EL Elemental Analyser (Elementar, Germany). A total of 150 mL of samples were collected and heated in a water bath at 60 °C for 30 min, and then centrifuged for 20 min at 15000*g* to exclude extracellular polymeric substances (EPS) (Xu et al., 2013b). After discarding the supernatant, the pellets were stored at −20 °C. Before analysis, the pellets were dipped in 1 M of HCl for 16 h in a chamber to remove inorganic C and then dried at 60 °C.

Particulate organic P was measured using a wet-oxidation method, as described by Aspila et al. (1976). Duplicate samples of 5 mL were filtered through a single pre-combusted (400 °C, 4 h) MF 300 filter (25 mm glass microfiber 0.70-μm pore size; Whatman Inc., UK). One was digested with potassium persulphate and autoclaved for analyzing particulate total P (PTP). The other one was dipped in 1 M HCl for 24 h and shaken 4 times for analyzing particulate inorganic P (PIP). The difference between PTP and PIP was POP.

2.2.4. Enzyme activities

The activities of carbonic anhydrase (CA) and nitrate reductase (NR) were analyzed by double-antibody sandwich enzyme-linked immunosorbent assays (ELISAs) based on the specific interaction between an antibody and the corresponding antigen, using a microbiological ELISA kit (Naning SenBeiJia Biological Technology Co., Ltd., China) based on the standard protocol. Alkaline phosphatase (AP) activity was measured using a modified procedure Chróst and Overbeck (1987). Bulk 3 mL samples were incubated at 25 °C for 3 h in the presence of a 0.05-mM Tris-HCl buffer (pH = 8.5) and 2-mL 0.3 mM *p*-nitronphenyl phosphate (p-NPP) as a substrate; subsequently, 100 μL of 0.1 M NaOH was added into the mixture after 3 h. The release of p-nitrophenol from p-NPP was determined by absorbance at 410 nm using a spectrophotometer (TU-1901, Puxi, China), and AP activity was calculated at μmol/h · 10^6 cells.

2.2.5. Extracellular polymeric substances

Extraction of EPSs was conducted via the process described by Xu et al. (2013a). In this study, the EPS matrix was classified as soluble EPS (SL-EPS) and bound EPS. The former represents the fraction that could be removed by slow centrifugation, and the latter displays a dynamic double-layered structure, which can be further divided into loosely bound EPS (LB-EPS) and tightly bound EPS (TB-EPS) (Li and Yang, 2007; Sheng et al., 2010; Xu et al., 2010). Ten milliliters of collected samples were first centrifuged at 2500 ×*g* for 15 min, and the supernatant was collected for measurement of SL-EPS. Second, the harvested algae samples were suspended in a 0.05% NaCl solution and centrifuged at 5000 ×*g* for 15 min. The liquid was collected carefully for measurement of LB-EPS. Third, the remaining algae samples were resuspended with a 0.05% NaCl solution and then heated at 60 °C for 30 min. The extracted solutions were centrifuged at 15000 ×*g* for 20 min, with the supernatant as the TB-EPS fraction. Additionally, 5 mL of collected samples were directly heated at 60 °C for 30 min and then centrifuged at 15000 ×*g* for 20 min to determine the total EPS. Finally, all of the EPS fractions were filtered using 0.45-mm polytetrafluoroethylene (PTFE) membranes (Xingya Purification Materials Co., China), and the solution was filtered for fluorescence after diluting it 10 times.

The content of the total EPS was characterized by the total organic carbon (TOC) using liquid TOC II (Elementar, Germany). Additionally, the polysaccharides, proteins, and deoxyribonucleic acid (DNA) in each EPS fraction were measured. Polysaccharide content was determined using phenol-sulfuric acid (Dubois et al., 1980) using glucose as a standard. Protein content was determined according to the methods of Bradford (1976). The DNA content was measured using a diphenylamine colorimetric method (Burton, 1956) with fish sperm and Na salt as the standards.

2.3. Statistical analyses

Data were analyzed using the IBM SPSS 19.0 (IBM, USA) statistical program. Histograms, line graphs, and scatter plots were generated using Sigma Plot 10.0 (Systat Software, USA).

3. Results

3.1. Improved growth rate of *M. aeruginosa* in response to elevated CO_2

Cells exposed to elevated CO_2 conditions occurred in a higher density at the end of cultivation (Fig. 1 and Table S1), indicating that

elevated CO_2 promoted the growth rate of *M. aeruginosa* regardless of nutrient levels. This result was consistent with the study of (Pierangelini et al., 2014), where the cell-specific division rate of *Cylindropermopsis raciborskii* at 1300 ppm CO_2 was 10% higher than that at 400 ppm CO_2. With the growth of *M. aeruginosa*, the pH of the cultures varied (Fig. 2). In the beginning, pH increased rapidly from 7.5 to ~10, and then remained at this level. However, after 16 days, the pH in PM and PH treatments gradually decreased to 7.5. Meanwhile, it was noted that with decreased pH, the increase rate of cell density became smaller and even negative after 16 days. Meanwhile, nitrate and phosphate concentration has declined below 0.5 mg/L and 0.15 mg/L respectively (Figs. S1 and S2).

3.2. Changes in the quantum yields of PSII and dark respiration with elevated CO_2

The light utilization efficiency of PSII in *M. aeruginosa* was enhanced by elevated CO_2. As shown in Fig. 3(a), cells cultured under elevated CO_2 conditions showed an increase in F_v/F_m, though no significant difference was observed between the 1100 ppm and 2200 ppm CO_2 treatments. Similarly, Y(II) were also higher in the media with higher CO_2 concentrations than those with low CO_2 (Fig. 3(b)). Moreover, *M. aeruginosa* grown in both nutrient-rich and nutrient-poor media displayed increased NPQ and Y(NPQ), but decreased in Y(NO) as the CO_2 concentration increased (Fig. 3(a, b)). As a result, extremely low ratios of Y(NPQ) and Y(NO) were found in RL (0.000) and PL (0.003) and higher values occurred with elevated CO_2 (0.061 in RM, 0.119 in RH, 0.052 in PM, and 0.049 in PH). It was notable that these parameters of PSII, including F_v/F_m, Y(II), and the ratio of Y(NPQ) to Y(NO), increased more in nutrient-rich media than in nutrient-poor media with elevated CO_2. Additionally, these parameters in PM and PH were higher than those in RL. Higher CO_2 values also had strong impacts on the dark respiration of *M. aeruginosa* (Fig. 3(c)). It was clear that dark respiration declined in higher CO_2 treatments, though there was no difference between 1100 ppm and 2200 ppm CO_2.

3.3. Effect of elevated CO_2 on cell composition

The cellular organic matter quotas of *M. aeruginosa* were also examined for changes under elevated CO_2 and nutrient conditions. Under nutrient-rich conditions, the POC/PON ratio of *M. aeruginosa* was ~6, which is lower than the Redfield C/N ratio (6.6). In contrast, under

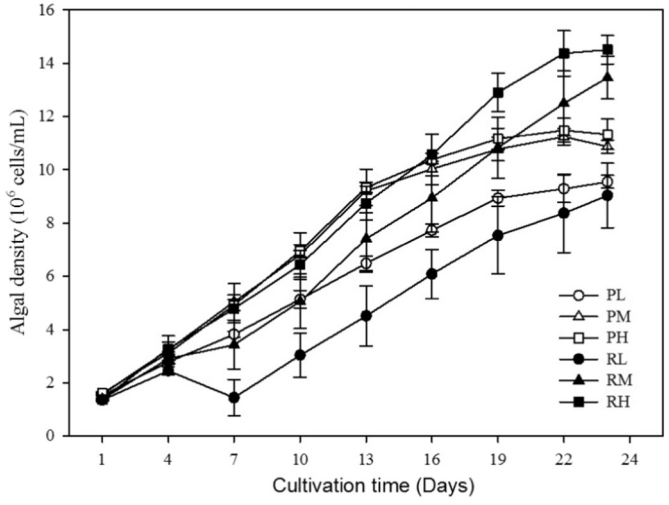

Fig. 1. Variation in the growth of *Microcystis aeruginosa* FACHB-927 in different treatments. (PL, nutrient-poor conditions with 400 ppm CO_2; PM, nutrient-poor conditions with 1100 ppm CO_2; PH, nutrient-poor condition with 2200 ppm CO_2; RL, nutrient-rich conditions with 400 ppm CO_2; RM, nutrient-rich conditions with 1100 ppm CO_2; RH, nutrient-rich conditions with 2200 ppm CO_2).

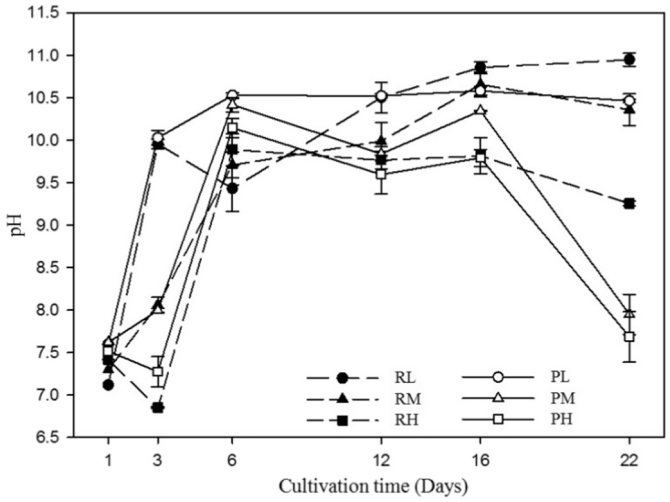

Fig. 2. Change in pH of the cultivation medium of *M. aeruginosa* under different treatment conditions (RL, nutrient-rich conditions with 400 ppm CO_2; RM, nutrient-rich conditions with 1100 ppm CO_2; RH, nutrient-rich conditions with 2200 ppm CO_2; PL, nutrient-poor conditions with 400 ppm CO_2; PM, nutrient-poor conditions with 1100 ppm CO_2; PH, nutrient-poor condition with 2200 ppm CO_2).

nutrient-poor conditions, the value remained higher, at ~8. Further, it was observed that POC/PON under nutrient-poor conditions showed an upward trend, while under nutrient-rich conditions, it displayed a downward trend (Fig. 4(a)). The POP of cells exposed to abundant nutrients was dramatically higher than that of cells with poor nutrient supplies ($p < 0.05$, Fig. 4(b)). With increasing CO_2, the PIP of *M. aeruginosa* increased and POP decreased in nutrient-rich media. Conversely, a slight increase in POP was observed in nutrient-poor media, though there was no statistical difference ($p = 0.193$).

Microcystis aeruginosa grown at different CO_2 concentrations and nutrient levels displayed clear difference in the EPSs. In this study, detailed analyses were conducted on the contents and components of the algal EPS. The total content of EPS was characterized by TOC. In cultures with abundant nutrients, the EPS of *M. aeruginosa* decreased with elevated CO_2 with respect to TOC, polysaccharides, protein, and DNA (Fig. 5). In contrast, TOC in the EPS of *M. aeruginosa* increased with elevated CO_2 under nutrient-poor conditions (PL = 2.77, PM = 3.25, and PH = 3.52 μg/cell). However, polysaccharides in EPS did not show uniform response to elevated CO_2, decreasing from PL to PM but increasing at PH. Protein decreased but DNA increased under higher CO_2 conditions, although it was not statistically significant.

As shown in Fig. 6(a), the polysaccharide ratio showed an increase with the TOC of EPSs in nutrient-poor media. In contrast, the polysaccharide ratio declined with TOC in nutrient-rich media. Polysaccharides and proteins were indicated as the main components in every fraction of EPS in all of the different treatments (Fig. 5), in accordance with Xu et al. (2013b). However, the proportion of polysaccharides and proteins varied with different treatments (Fig. 6(b)). The polysaccharide/protein ratio in all of the EPS (total) remained stable with elevated CO_2 under nutrient-rich conditions (RL = 1.01, RM = 1.05, and RH = 1.05), but continued rising under nutrient-poor conditions (PL = 1.17, PM = 1.37, and PH = 1.76). Additionally, the ratio under PL and PH conditions was much higher than under nutrient-rich conditions ($p < 0.05$).

3.4. Effect of elevated CO_2 on enzyme activity

Different enzyme activities exhibited a non-uniform response to elevated CO_2. The change in carbonic anhydrase (CA) differed between nutrient-rich and nutrient-poor media (Fig. 7(a)); decreasing under nutrient-rich conditions as CO_2 increased, with RL = 9.87, RM = 7.32, and RH = 6.83 nmol/min · 10^6 cells. However, there was no obvious change in CA activity under nutrient-poor conditions ($p > 0.05$),

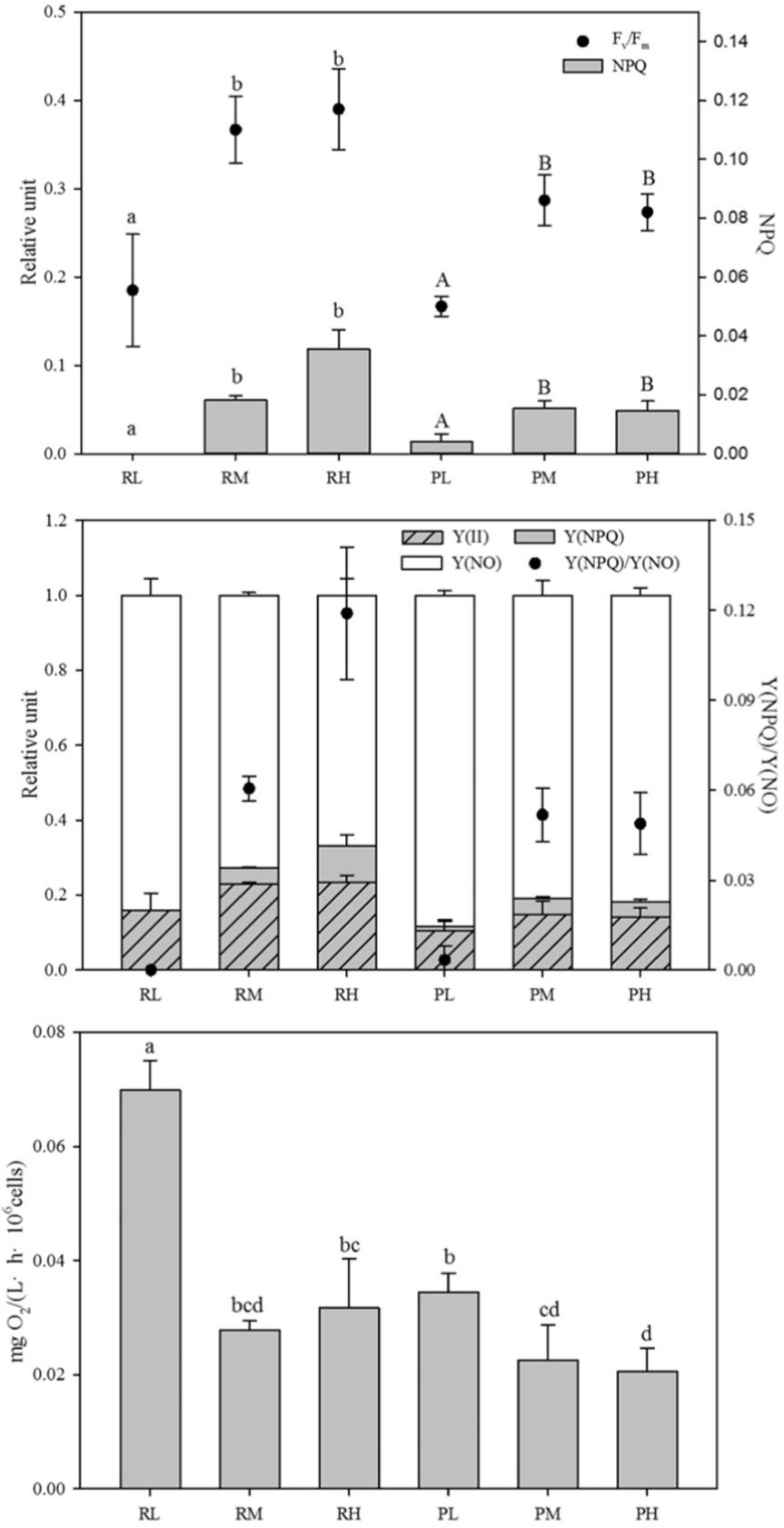

Fig. 3. (a) Maximum photochemical quantum yield (F_v/F_m) and non-photochemical quenching (NPQ); (b) photochemical quantum yield (Y(II)), quantum yield of light-induced (Y(NPQ)) and non-regulated heat dissipation and fluorescence emissions (Y(NO)); (c) dark respiration rate in different treatments. Different lowercase letters in superscription indicate significant differences ($p < 0.05$) among nutrient-rich treatments, and capital letters in superscription indicate significant differences ($p < 0.05$) among nutrient-poor treatments. (PL, nutrient-poor conditions with 400 ppm CO_2; PM, nutrient-poor conditions with 1100 ppm CO_2; pH, nutrient-poor condition with 2200 ppm CO_2; RL, nutrient-rich conditions with 400 ppm CO_2; RM, nutrient-rich conditions with 1100 ppm CO_2; RH, nutrient-rich conditions with 2200 ppm CO_2).

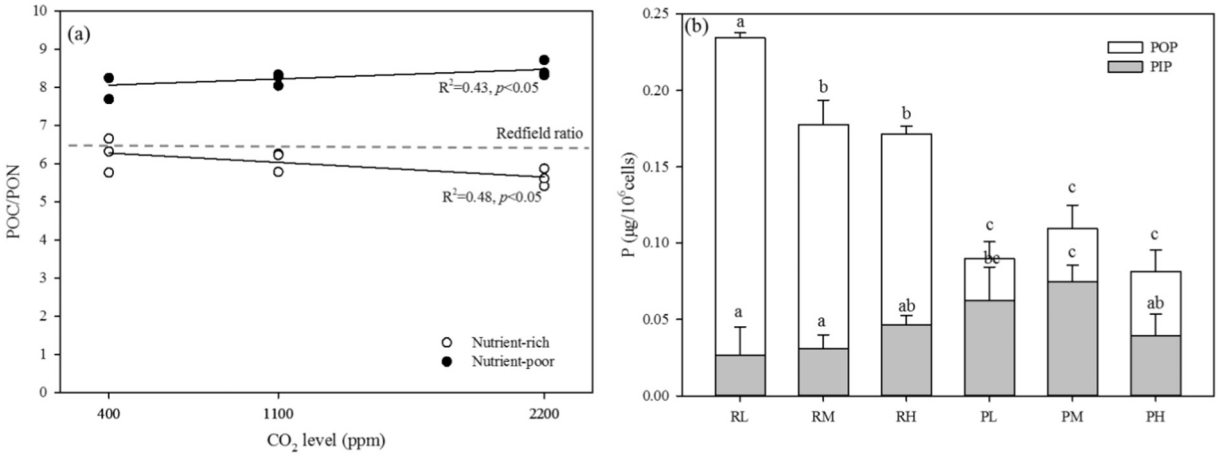

Fig. 4. (a) Correlation of particulate organic carbon (POC)/particulate organic nitrogen (PON) with CO_2 levels at different nutrient levels. (b) particulate organic phosphorus (POP) and particulate inorganic phosphorus (PIP) of *M. aeruginosa* in different treatments. Different letters in superscription indicate significant differences ($p < 0.05$) among treatments.

where CA activity remained relatively high (Fig. 7(a)). The effect of CO_2 on NR activity was similar at different nutrient levels. The highest NR activity was found at 400 ppm CO_2 (Fig. 7(a); RL = 1.28 nmol/min · 10^6 cells and PL = 1.44 nmol/min · 10^6 cells). As CO_2 rose, a decrease in NR activity was observed ($p < 0.05$ in nutrient-rich media and $p > 0.05$ in nutrient-poor media), accompanied by reduced NO_3^- assimilation ($p > 0.05$ in nutrient-rich media and $p < 0.05$ in nutrient-poor media, Fig. 7(b)). Alkaline phosphatase was only detected under nutrient-poor conditions, and exhibited a maximum rate of 3.02 nmol p-NPP of 10^6 cells/h at 2200 ppm CO_2. Meanwhile, the AP activities at 400 ppm (2.17 nmol/h · 10^6 cells) and 1100 ppm (1.93 nmol/h · 10^6 cells) were 36% and 28% lower, respectively, than at 2200 ppm CO_2 (Fig. 7(a)).

4. Discussion

Elevated CO_2 was able to increase the growth rate and population density of *M. aeruginosa*, especially in nutrient-rich media. Similarly, the growth rate of many other phytoplankton, like dinoflagellates and diatoms, may also be promoted by elevated CO_2 (Federico and Mario, 2010; Yang and Gao, 2012). These findings suggested that CO_2 is commonly a limiting factor for algal growth. In nutrient-saturated cultures, the phytoplankton biomass was doubled at 1200 ppm of CO_2, compared with that at 200 ppm CO_2 (Verspagen et al., 2014b). Field evidence for the response of cyanobacterial blooms to elevated CO_2 is limited, but in a large-scale comparative study of 69 boreal lakes, it was found that

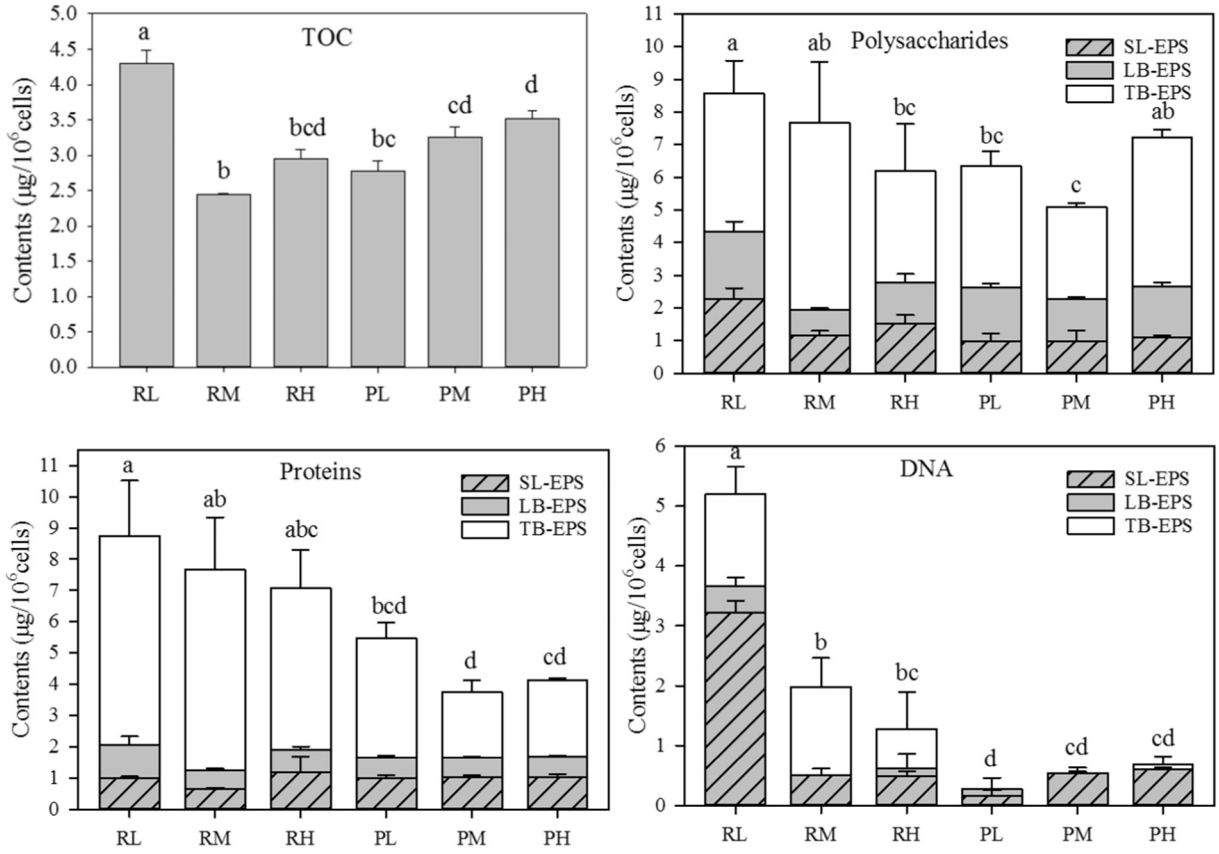

Fig. 5. Total organic carbon (TOC), polysaccharides, proteins, and deoxyribonucleic acid (DNA) in the extracellular polymeric substance (EPS) of *M. aeruginosa* in different treatments. Different letters in superscription indicate significant differences ($p < 0.05$) among treatments.

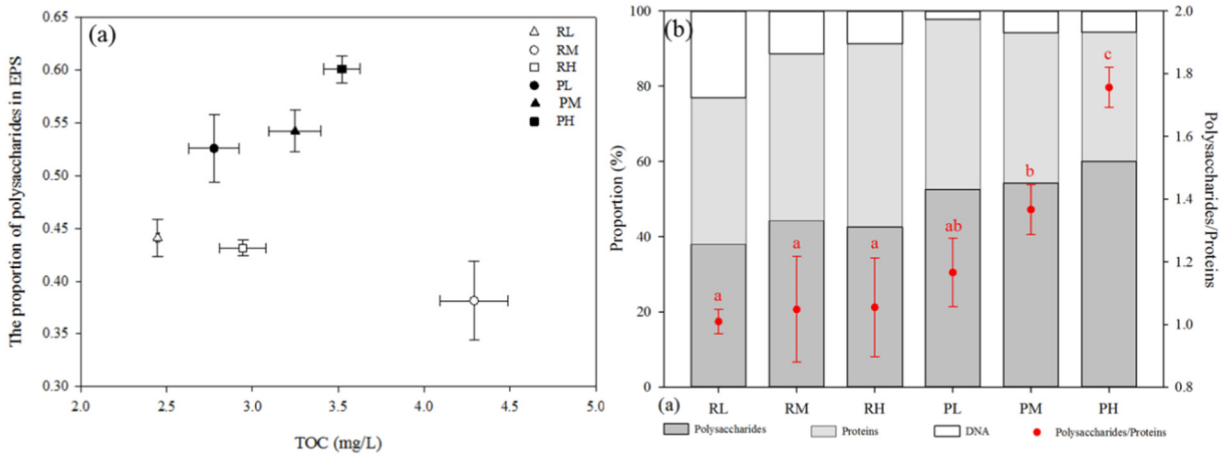

Fig. 6. (a) Relationship between TOC and the proportion of polysaccharides in EPS; (b) proportion of polysaccharides (dark fill), proteins (light fill), and DNA (white fill) in EPS (histogram) and the proportion of polysaccharides and proteins (scatters) in different treatments of *M. aeruginosa*. Different letters in superscription indicate significant differences ($p < 0.05$) among treatments.

phytoplankton primary productivity (PP) was significantly and positively correlated with the partial pressure of carbon dioxide (pCO_2; Vogt et al., 2017). Moreover, in a microcosm experiment in Meiliang Bay, Lake Taihu, a 65% increase in PP was observed after being treated with 750 ppm of CO_2 (Shi et al., 2016). However, in the less eutrophic eastern area of Lake Taihu, PP was only slightly promoted after the same treatment (Shi et al., 2017). Similarly, there is a significant but small stimulation of PP (15–19%) in response to elevated CO_2 in the nutrient-poor Atlantic Ocean (Hein and Sand-Jensen, 1997), which implies that the stimulation of PP from elevated CO_2 may be related to nutrient levels, and the growth of cyanobacteria are less likely to be promoted by rising CO_2 in oligotrophic waters (Verspagen et al., 2014a).

In this study, the population densities of *M. aeruginosa* in both nutrient-rich and nutrient-poor media increased with elevated CO_2. However, a decline occurred in nutrient-poor media by the end of the experiment. Improved growth at elevated CO_2 leads to the depletion of nutrients (Verschoor et al., 2013). Therefore, phytoplankton biomass was initially promoted by elevated CO_2. However, when the nutrients were depleted, phytoplankton biomass would decreased, irrespective of the CO_2 treatment (Riebesell et al., 2007). It is agreed that N and P availability exert strong controls on algal growth, and this may modify the physiological responses of *M. aeruginosa* to elevated CO_2.

4.1. Improved energy transfer in PSII under elevated CO_2 conditions

In many studies, it has been demonstrated that PSII is one of the most sensitive target sites for environmental stress (Wang et al., 2014). For example, chilling temperature and heavy metals can inhibited activities of PSII (Wei et al., 2010; Wang et al., 2014). However, few studies have been focused on the influence of elevated CO_2 on PSII in cyanobacteria. In this study, it was observed improved energy transfer in PSII under elevated CO_2 conditions. One line of evidence for this was the higher F_v/F_m and Y(II) at medium and high CO_2 concentrations, suggesting that elevated CO_2 improved the utilization efficiency of light energy. In another cyanobacterium, *Cylindrospermopsis raciborskii*, a twice higher maximum light for photosynthesis has been observed under 1300 ppm CO_2 conditions than that under 400 ppm CO_2 conditions (Pierangelini et al., 2014). These changes could be attributable to downregulated CCM. Yang and Gao (2012) found that cells exposed to low CO_2 and high CO_2 levels exhibited equal amounts of electron transfer, but fewer electrons were used for carboxylation in the low-CO_2 grown cells. This result suggests that under high CO_2 conditions, fewer extra electrons are expended to operate the CCM. Additionally, NPQ in this study increased with elevated CO_2. NPQ is an important mechanism, which protects cells from photo damage and minimizes the production of harmful oxygen radicals (Niyogi et al., 2005). The results in

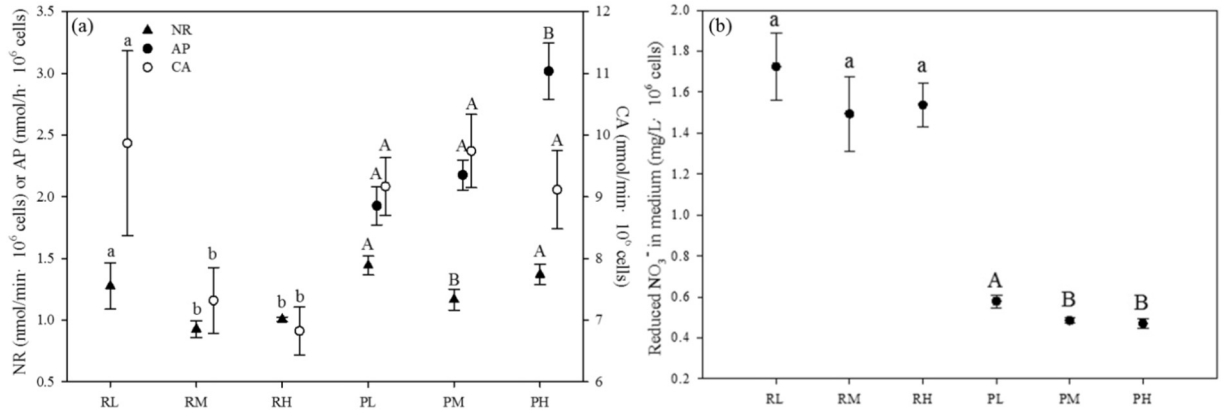

Fig. 7. (a) Activity of carbonic anhydrase (CA), nitrate reductase (NR), and alkaline phosphatase (AP) in different treatments; (b) reduced NO_3^- in the media of different treatments. Different lowercase letters in superscription indicate significant differences ($p < 0.05$) among nutrient-rich treatments, and capital letters in superscription indicate significant differences ($p < 0.05$) among nutrient-poor treatments. (PL, nutrient-poor conditions with 400 ppm CO_2; PM, nutrient-poor conditions with 1100 ppm CO_2; PH, nutrient-poor condition with 2200 ppm CO_2; RL, nutrient-rich conditions with 400 ppm CO_2; RM, nutrient-rich conditions with 1100 ppm CO_2; RH, nutrient-rich conditions with 2200 ppm CO_2).

this study suggested that photoprotection in *M. aeruginosa* was enhanced.

Higher NPQs suggest the increasing dissipation of excessive light energy (Kramer et al., 2004). Elevated CO_2 is supposed to relax NPQ under high light conditions because of improved light utilization (Shimakawa et al., 2016). However, downregulated CCM under elevated CO_2 conditions could be associated with weakened cyclic electron transport, which can also lead to higher photoinhibition (Shunichi et al., 2009). It has been demonstrated that when high-CO_2 grown cells are transferred back to low-CO_2 media, their photoinhibition of the electron transport rate (ETR) decreased due to activation of the CCM (Wu et al., 2010). Overall, the increased NPQ of *Microcystis aeruginosa* in our study may be an integrated result. The result is caused by enhanced photoinhibition by downregulated CCM exceeding improved light utilization. Conversely, a decrease in NPQ of a marine diatom *Phaeodactylum tricornutum* has been observed under elevated CO_2 (Wu et al., 2010), which represented a net result of the improved light utilization exceeding enhanced photoinhibition. These results suggested that the changed NPQ may be species-specific. It depends on the degree of both downregulated CCM and improved light utilization of the species studied.

Genty et al. (1996) demonstrated that the absorbed excitation energy in PSII is partitioned into three fundamental pathways: charge separation to accomplish photochemical reaction (Y(II)), regulating energy losses of excitation energy via heat dissipation (Y(NPQ)), and non-regulated losses of excitation energy, including heat dissipation and fluorescence emission (Y(NO)). The increase in Y(II) was mainly due to the decreased Y(NO), and a much higher ratio of Y(NPQ) to Y(NO) indicates that excess excitation energy fluxes can be safely dissipated at the antenna level, which is what occurred in *M. aeruginosa* with elevated CO_2 (PM, PH, RM, and RH). In contrast, extremely low ratios of Y(NPQ) to Y(NO) occurred in PL and RL, meaning that PSII of *M. aeruginosa* at low CO_2 concentrations was damaged.

As expected, the light utilization efficiency and photoprotection of PSII were improved by elevated CO_2, particularly in nutrient-rich media, because ample nutrient supplies help cells to accumulate large pools of conserved protein complexes for using light and resisting damage (Li et al., 2015). Nitrogen and P are essential in protein synthesis and ATP, which is itself necessary in photosystem (Hipkin et al., 1983, Li et al., 2015). Diatoms cultivated in N-limited chemostats have been found to conduct lower rates of photosynthesis (Hennon et al., 2014). This finding suggests that the positive effect of elevated CO_2 may disappear under depleted nutrient conditions, and even turn to negative.

4.2. Higher carbon/nutrient ratio caused by elevated CO_2 under nutrient-limited conditions

Elemental stoichiometric ratios in algae are of interest due to their role in reflecting food quality and predicting biogeochemical variations (Hennon et al., 2017). Some previous studies reported that increased C/nutrient ratio with rising CO_2, while other studies did not show an increase in C/nutrient stoichiometry. One explanation for this is that there are species-specific responses and acclimation trajectories (Hennon et al., 2017). The other explanation attributes these conflicting results to varying nutrient levels (Verspagen et al., 2014a). In the chemostat study of Verspagen et al. (2014a), a range of different gas-flow CO_2 concentrations was set, from 0.5 to 2800 ppm. In the chemostats supplied with high N loads, the molar POC/PON ratio of *M aeruginosa* remained low, irrespective of CO_2. In contrast, in chemostats supplied with low N loads, the molar POC/PON ratio increased to ~14 at $CO_2 > 100$ ppm. The results of our study were consistent with patterns in the range of 400–2800 ppm CO_2 observed by Verspagen et al. (2014a). These findings confirmed that changes in the elemental stoichiometric ratios depend on CO_2 only when nutrient loads are low.

In addition to the molar POC/PON ratio, heterogeneous components in the EPSs of different treatments also revealed that the effect of CO_2 on cell composition is nutrient-related. Extracellular polymeric substances are composed mainly of polysaccharides, proteins, humic substances, and other biological macromolecules (Xu et al., 2014). In nutrient-poor media, EPS increased with elevated CO_2. Moreover, EPS serves as a sink for overflows in carbon metabolism (Xu et al., 2013a). Studies have reported that nitrogen- or P-starvation or low levels of nutrients could lead to an increase in EPS production (Huang et al., 2007, Otero and Vincenzini, 2004). Under these conditions, fixed C would be more redundant, which was then diverted to the support the production of exopolysaccharides (Otero and Vincenzini, 2004). This explains the positive relationship between TOC in EPS and the polysaccharide ratio. In contrast, in nutrient-rich media, the highest TOC and polysaccharide ratios were observed in RL. It was clear that the high TOC was not caused by excessive C metabolism, as TOC was negatively correlated with the polysaccharide ratio. Elevated CO_2 in nutrient-rich media primarily acted to balance the synthesis of N-rich and P-rich molecules in cells.

Carbohydrate-to-protein ratios have been demonstrated to be useful indicators of the nutritional status of cyanobacterial cells (Otero and Vincenzini, 2004). In this study, there was an increase in the polysaccharides/protein ratio of EPS with elevated CO_2 in nutrient-poor media, indicating that cells were N-limited. Additionally, the ratio was much higher than in nutrient-rich media. These results were consistent with the POC/PON ratio, which was high under nutrient-poor conditions but low under nutrient-rich conditions. Such changes implied the reduced nutritional quality of phytoplankton in nutrient-limited media (Sterner and Elser, 2002). Extrapolation from the results to a natural ecosystem indicates that in oligotrophic waters, rising atmospheric CO_2 will increase carbon/nutrient ratios, and possibly alter the structure of food webs.

4.3. Facilitated intracellular acidification by high CO_2 under nutrient-poor conditions

The typical cyanobacteria CCM is based on the uptake of CO_2 and bicarbonate from the environment, and the conversion of them is closely related to CA. In this study, decreased CA was only observed in nutrient-replete media with elevated CO_2; CA was divided into extracellular CA and intracellular CA. Extracellular CA mainly converts HCO_3^- to CO_2, generating an inward diffusive CO_2 gradient to the cell (Jansson and Northen, 2010). Intracellular CA converts HCO_3^- to CO_2 to maintain a high level of CO_2 around carboxysomes (Visser et al., 2016), meanwhile acting to minimize CO_2 loss from the cell by converting CO_2 to HCO_3— (Chrachri et al., 2018). These processes are important in regulating cellular pH by the release or consumption of hydrogen ions (Jansson and Northen, 2010).

Elevated CO_2 can alleviate the transformation of HCO_3^- to CO_2 at the cell surface, leading to a lower CA activity and a higher pH (Chrachri et al., 2018). The CO_2 diffusing into a cell was effectively utilized for photosynthesis in nutrient-rich media, which could be suggested by improved light utilization of photosynthesis (see Section 4.1). However, photosynthesis was weakened when nutrients were limited, which can be demonstrated by the lower F_v/F_m and Y(II) in PM and PH relative to RM and RH. It suggested that cells in nutrient-poor media have a reduced ability to use additional CO_2. In this case, they are likely to convert CO_2 to HCO_3^- for storage (Fig. 8(d)), resulting in a higher CA level (Fig. 4(a)) and a declining pH (Fig. 2). This explains the reduced CA activity in nutrient-rich media as CO_2 rises, as well as the relatively high CA activity in nutrient-poor media irrespective of CO_2 treatments. Moreover, it suggests that under long-term, elevated CO_2 conditions, CA may be the important contributor to intracellular acidification. Extrapolation the results to natural ecosystem indicates that in future high-CO_2 conditions, cyanobacteria in mesotrophic and eutrophic waters are less likely get influenced by acidification, as they are able to make use of the increased CO_2. However, due to cyanobacteria in oligotrophic waters possibly losing the ability to use excessive CO_2, they are more likely to suffer intracellular acidification. The intracellular acidification will then inhibit the growth of cyanobacteria by affecting protoplasmic ion balance and

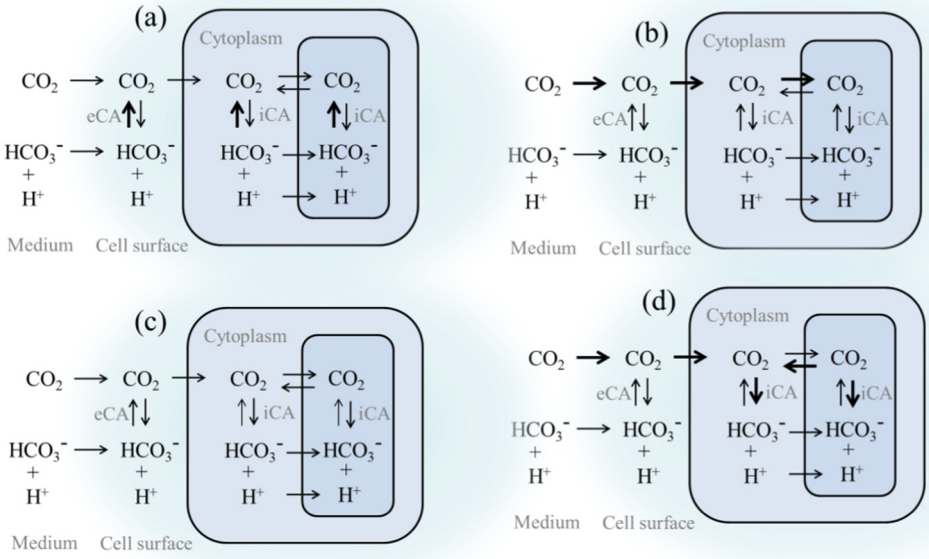

Fig. 8. Cellular modelling of carbonate chemistry surrounding and in *M. aeruginosa* cells under different conditions. (a) Low CO_2 with abundant nutrients; (b) elevated CO_2 with abundant nutrients; (c) low CO_2 without abundant nutrients; (d) elevated CO_2 without abundant nutrients. The increasing thicknesses of the arrows indicate process enhancement.

damaging photosynthetic system (Wang et al., 2011; Yang et al., 2018). Consequently, decreased productivity will occur accompanied by acidification and aquatic ecosystems may lose the balance.

4.4. The influence of changed enzyme activity on nutrient uptake under elevated CO_2 conditions

There are few studies concerning the effects of rising CO_2 on the enzymes involved in N and P uptake. Alkaline phosphatase is an important enzyme in the utilization of dissolved organic P, and it can be induced by low dissolved inorganic P in cells (Endres et al., 2013). In this study, PIP was lowest in PH, and the AP activity increased with increasing CO_2 conditions in nutrient-poor media. This implied that *M. aeruginosa* improved its ability for DOP utilization as CO_2 increased. Similar results has been observed in the study of Endres et al. (2013), where the AP activity of cyanobacterium *Nodularia spumigena* also increased with increased CO_2. Stimulated growth of cyanobacteria by high CO_2 may raise its demand for phosphorus, thus increasing the expression of more AP. Besides, reduced pH by elevated CO_2 could be another important factor in regulating AP activity. In this study, the pH values remained optimal for AP (~7.5–10) (Healey and Hendzel, 2010; Münster et al., 1992); thus, AP activity was not inhibited by elevated CO_2. The results tended to be completely different when CO_2 reduced the pH below the optimum threshold. For example, AP activity was initially improved by the elevated CO_2 concentration, but was inhibited when CO_2 concentration continued to increase (Rouco et al., 2013). This indicates that AP activity may be suppressed if intracellular acidification continues. Nonetheless, the ability for DOP utilization of cyanobacteria could improve by elevated CO2, providing that reduced pH remains in the optimum range for AP.

Elevated CO_2 inhibited the NR activity and nitrate assimilation in this study, irrespective of nutrient levels. A similar pattern emerged in another phytoplankton, *T. pseudonana* (Shi et al., 2015). The inhibited NR activity was concurrent with reduced NR gene transcription and protein expression at high CO_2 concentrations (Shi et al., 2015). Interestingly, the inhibition of N metabolism by elevated CO_2, like suppressed NO_3^- assimilation, has been reported in some terrestrial C_3 plants and results in lower protein content (Bloom, 2014; Myers et al., 2014). This is a phenomenon that should be of concerns for aquatic systems, although reduced protein contents were not been found in this study or in *T. pseudonana*. However, the cultivation period was less than one month and long-term elevated CO_2 conditions may impact protein content. Additionally, the underlying mechanism responsible for the high-CO_2 inhibition of NO_3^- assimilation remains largely unknown. One possible explanation is the down-regulation of key iron-binding proteins (i.e., AfuA, FhuC, and FhuD) under elevated CO_2, since it decreases intracellular iron, which is contained in the NR active site (Wan et al., 2016), thus reducing the NR activity. Changes in AP and NR activity suggest that elevated atmospheric CO_2 influences primary producers, not only through direct effects on carbon fixation, but also through nutrient uptake and utilization.

5. Conclusions

Our study demonstrates that cyanobacteria vary in their response to elevated atmospheric CO_2 over a range of nutrient levels. These findings can provide physiological explanations for altered growth of cyanobacteria under rising atmospheric CO_2 conditions. Cyanobacteria improved their light utilization efficiency and the photoprotection of PSII under elevated CO_2 conditions, particularly when cells were supplied with abundant nutrients. However, only cyanobacteria experiencing nutrient deprivation increased their polysaccharides/protein ratio of EPS with elevated CO_2, resulting in poor food quality. Besides, cyanobacteria under such conditions were more likely to suffer intracellular acidification. Nonetheless, the ability for DOP utilization of cyanobacteria could get improved by high CO_2, provided that reduced pH is still in the optimum range for AP. These findings suggest that investigations into the influence of increasing atmospheric CO_2 on algae should take into account the nutrient levels of the ecosystems being examined. In eutrophic and hypertrophic waters, cyanobacteria may benefit from elevated atmospheric CO_2, thus intensifying cyanobacterial blooms. Conversely, in oligotrophic waters, elevated CO_2 would result in poor food quality and decreased primary productivity.

Acknowledgements

This work was supported by the National Natural Science Foundation of China [No. 51579073]; the National Major Projects of Water Pollution Control and Management Technology (No. 2017ZX07204003); the National Science Funds for Creative Research Groups of China [No. 51421006]; the Key Program of National Natural Science Foundation of China (No. 91647206).

Appendix A. Supplementary data

Supplementary data to this article can be found online at https://doi.org/10.1016/j.scitotenv.2019.07.056.

References

Aspila, K.I., Agemian, H., Chau, A.S., 1976. A semi-automated method for the determination of inorganic, organic and total phosphate in sediments. Analyst 101, 187–197.
Beversdorf, L.J., Miller, T.R., Mcmahon, K.D., 2015. Long-term monitoring reveals carbon-nitrogen metabolism key to microcystin production in eutrophic lakes. Front. Microbiol. 6, 456.
Bloom, A.J., 2014. Photorespiration and nitrate assimilation: a major intersection between plant carbon and nitrogen. Photosynth. Res. 123.
Boyd, P.W., Hutchins, D.A., 2012. Understanding the responses of ocean biota to a complex matrix of cumulative anthropogenic change. Mar. Ecol. Prog. Ser. 470, 125–135.
Bradford, M.M., 1976. A rapid and sensitive method for the quantitation of microgram quantities of protein utilizing the principle of protein-dye binding. Anal. Biochem. 72, 248–254.
Brennan, G.L., Collins, S., 2015. Growth responses of a green alga to multiple environmental drivers. Nat. Clim. Chang. 3478, 127–141.
Burton, K., 1956. A study of the conditions and mechanism of the diphenylamine reaction for the colorimetric estimation of deoxyribonucleic acid. Biochem. J. 62, 315–323.
Chrachri, A., Hopkinson, B.M., Flynn, K., Brownlee, C., Wheeler, G.L., 2018. Dynamic changes in carbonate chemistry in the microenvironment around single marine phytoplankton cells. Nat. Commun. 9, 74.
Chróst, R.J., Overbeck, J., 1987. Kinetics of alkaline phosphatase activity and phosphorus availability for phytoplankton and bacterioplankton in lake plu\see (North German Eutrophic Lake). Microb. Ecol. 13, 229–248.
Cole, J.J., Caraco, N.F., Kling, G.W., Kratz, T.K., 1994. Carbon dioxide supersaturation in the surface waters of lakes. Science 265, 1568–1570.
Conley, D.J., Paerl, H.W., Howarth, R.W., Boesch, D.F., Seitzinger, S.P., Havens, K.E., Christiane, L., Likens, G.E., 2009. Controlling eutrophication: nitrogen and phosphorus. Science 323, 1014.
Dubois, M., Gilles, K.A., Hamilton, J.K., Rebers, P.A., Smith, F., 1980. Colorimetric method for determination of sugars and related substances. Anal. Chem. 89, 449–454.
Endres, S., Unger, J., Wannicke, N., Nausch, M., Voss, M., Engel, A., 2013. Response of the filamentous cyanobacterium Nodularia spumigena to pCO_2 - exudation and extracellular enzymes. Biogeosciences 10, 567–582.
Federico, M., Mario, G., 2010. Compositional homeostasis of the dinoflagellate Protoceratium reticulatum grown at three different pCO_2. J. Plant Physiol. 167, 110–113.
Genty, B., Harbinson, J., Cailly, A.L., Rizza, F., 1996. Fate of excitation at PS II in leaves: the non-photochemical side. The Third BBSRC Robert Hill Symposium on Photosynthesis, p. 28.
Hasler, C.T., Butman, D., Jeffrey, J.D., Suski, C.D., 2016. Freshwater biota and rising pCO_2? Ecol. Lett. 19, 98–108.
Healey, F.P., Hendzel, L.L., 2010. Fluorometric measurement of alkaline phosphatase activity in algae. Freshw. Biol. 9, 429–439.
Hein, M., Sand-Jensen, K., 1997. CO_2 increases oceanic primary production. Nature 388, 526–527.
Hennon, G.M., Quay, P., Morales, R.L., Swanson, L.M., Virginia Armbrust, E., 2014. Acclimation conditions modify physiological response of the diatom *Thalassiosira pseudonana* to elevated CO_2 concentrations in a nitrate-limited chemostat. J. Phycol. 50, 243–253.
Hennon, G.M.M., Hernandez Limon, M.D., Haley, S.T., Juhl, A.R., Dyhrman, S.T., 2017. Diverse CO_2-induced responses in physiology and gene expression among eukaryotic phytoplankton. Front. Microbiol. 8, 2547.
Hipkin, C.R., Thomas, R.J., Syrett, P.J., 1983. Effects of nitrogen deficiency on nitrate reductase, nitrate assimilation and photosynthesis in unicellular marine algae. Mar. Biol. 77, 101–105.
Huang, W.J., Lai, C.H., Cheng, Y.L., 2007. Evaluation of extracellular products and mutagenicity in cyanobacteria cultures separated from a eutrophic reservoir. Sci. Total Environ. 377, 214–223.
Jansen, E., Overpeck, J., Briffa, K., Duplessy, J.C., Joos, F., Masson-Delmotte, V., Olago, D., Otto-Bliesner, B., Peltier, W., Rahmstorf, S., Ramesh, R., Raynaud, D., Rind, D., Solomina, O., Villalba, R., Zhang, D., 2007. Climate Change 2007: The Physical Science Basis. Contribution of Working Group I to the Fourth Assessment Report of the Intergovernmental Panel on Climate Change. Cambridge University Press, Cambridge.
Jansson, C., Northen, T., 2010. Calcifying cyanobacteria-the potential of biomineralization for carbon capture and storage. Curr. Opin. Biotechnol. 21, 365–371.
Kramer, D.M., Johnson, G., Kiirats, O., Edwards, G.E., 2004. New fluorescence parameters for the determination of qaredox state and excitation energy fluxes. Photosynth. Res. 79, 209–218.
Lewis, E., Wallace, D., 1998. Program developed for CO_2 system calculations, Report, Carbon Dioxide Information Analysis Center. Oak Ridge National Laboratory.
Li, X.Y., Yang, S.F., 2007. Influence of loosely bound extracellular polymeric substances (EPS) on the flocculation, sedimentation and dewaterability of activated sludge. Water Res. 41, 1022–1030.
Li, G., Brown, C.M., Jeans, J.A., Donaher, N.A., Mccarthy, A., Campbell, D.A., 2015. The nitrogen costs of photosynthesis in a diatom under current and future pCO_2. New Phytol. 205 (2).
Liu, J., Van Oosterhout, E., Faassen, E.J., Lurling, M., Helmsing, N.R., Van de Waal, D.B., 2016. Elevated pCO_2 causes a shift towards more toxic microcystin variants in nitrogen-limited Microcystis aeruginosa. FEMS Microbiol. Ecol. 92.
Lorenzo, M.R., Iñiguez, C., Egge, J.K., Larsen, A., Berger, S.A., García-Gómez, C., Segovia, M., 2018. Increased CO_2 and iron availability effects on carbon assimilation and calcification on the formation of Emiliania huxleyi blooms in a coastal phytoplankton community. Environ. Exp. Bot. 148, 47–58.
Low-Decarie, E., Bell, G., Fussmann, G.F., 2015. CO_2 alters community composition and response to nutrient enrichment of freshwater phytoplankton. Oecologia 177, 875–883.
Maberly, S.C., 2010. Diel, episodic and seasonal changes in pH and concentrations of inorganic carbon in a productive lake. Freshw. Biol. 35, 579–598.
Mccarthy, A., Rogers, S.P., Duffy, S.J., Campbell, D.A., 2012. Elevated carbon dioxide differentially alters the photophysiology of *Thalassiosira pseudonana* (bacillariophyceae) and *Emiliania huxleyi* (haptophyta). J. Phycol. 48, 635–646.
Munday, P.L., Cheal, A.J., Dixson, D.L., Rummer, J.L., Fabricius, K.E., 2014. Behavioural impairment in reef fishes caused by ocean acidification at CO_2 seeps. Nat. Clim. Chang. 4 (6), 487–492.
Münster, U., Einiö, P., Nurminen, J., Overbeck, J., 1992. Extracellular enzymes in a polyhumic lake: important regulators in detritus processing. Hydrobiologia 229, 225–238.
Myers, S.S., Zanobetti, A., Kloog, I., Huybers, P., Leakey, A.D., Bloom, A.J., Carlisle, E., Dietterich, L.H., Fitzgerald, G., Hasegawa, T., Holbrook, N.M., Nelson, R.L., Ottman, M.J., Raboy, V., Sakai, H., Sartor, K.A., Schwartz, J., Seneweera, S., Tausz, M., Usui, Y., 2014. Increasing CO_2 threatens human nutrition. Nature 510, 139–142.
Niyogi, K.K., Li, X.P., Rosenberg, V., Jung, H.S., 2005. Is PsbS the site of non-photochemical quenching in photosynthesis? J. Exp. Bot. 56, 375–382.
O'Neil, J.M., Davis, T.W., Burford, M.A., Gobler, C.J., 2012. The rise of harmful cyanobacteria blooms: the potential roles of eutrophication and climate change. Harmful Algae 14, 313–334.
Otero, A., Vincenzini, M., 2004. Nostoc (cyanophyceae) goes nude: extracellular polysaccharides serve as a sink for reducing power under unbalanced C/N metabolism. J. Phycol. 40, 74–81.
Paerl, H.W., 1988. Nuisance phytoplankton blooms in coastal, estuarine, and inland waters. Limnol. Oceanogr. 33, 823–847.
Pierangelini, M., Stojkovic, S., Orr, P.T., Beardall, J., 2014. Elevated CO_2 causes changes in the photosynthetic apparatus of a toxic cyanobacterium, *Cylindrospermopsis raciborskii*. J. Plant Physiol. 171, 1091–1098.
Price, G.D., 2011. Inorganic carbon transporters of the cyanobacterial CO_2 concentrating mechanism. Photosynth. Res. 109, 47–57.
Reinfelder, J.R., 2012. Carbon dioxide regulation of nitrogen and phosphorus in four species of marine phytoplankton. Mar. Ecol. Prog. Ser. 466, 57–67.
Riebesell, U., Schulz, K.G., Bellerby, R.G.J., Botros, M., Fritsche, P., Meyerh?Fer, M., et al., 2007. Enhanced biological carbon consumption in a high CO_2 ocean. Nat. Clim. Chang. 450, 545–548.
Rokitta, S.D., John, U., Rost, B., 2012. Ocean acidification affects redox-balance and ion-homeostasis in the life-cycle stages of Emiliania huxleyi. PLoS One 7, e52212.
Rouco, M., Branson, O., Lebrato, M., Iglesias-Rodríguez, M.D., 2013. The effect of nitrate and phosphate availability on *Emiliania huxleyi* (NZEH) physiology under different CO_2 scenarios. Front. Microbiol. 4, 155.
Sandrini, G., Matthijs, H.C., Verspagen, J.M., Muyzer, G., Huisman, J., 2014. Genetic diversity of inorganic carbon uptake systems causes variation in CO_2 response of the cyanobacterium Microcystis. ISME J. 8, 589–600.
Sheng, G.P., Yu, H.Q., Li, X.Y., 2010. Extracellular polymeric substances (EPS) of microbial aggregates in biological wastewater treatment systems: a review. Biotechnol. Adv. 28, 882–894.
Shi, D., Li, W., Hopkinson, B.M., Hong, H., Li, D., Kao, S.-J., Lin, W., 2015. Interactive effects of light, nitrogen source, and carbon dioxide on energy metabolism in the diatom *Thalassiosira pseudonana*. Limnol. Oceanogr. 60, 1805–1822.
Shi, X., Zhao, X., Zhang, M., Yang, Z., Xu, P., Kong, F., Smith, R., 2016. The responses of phytoplankton communities to elevated CO_2 show seasonal variations in the highly eutrophic Lake Taihu. Can. J. Fish. Aquat. Sci. 73, 727–736.
Shi, X., Li, S., Wei, L., Qin, B., Brookes, J.D., 2017. CO_2 alters community composition of freshwater phytoplankton: a microcosm experiment. Sci. Total Environ. 607-608, 69–77.
Shimakawa, G., Akimoto, S., Ueno, Y., Wada, A., Shaku, K., Takahashi, Y., Miyake, C., 2016. Diversity in photosynthetic electron transport under [CO 2]-limitation: the cyanobacterium Synechococcus sp. PCC 7002 and green alga Chlamydomonas reinhardtii drive an O_2-dependent alternative electron flow and non-photochemical quenching of chlorophyll. Photosynth. Res. 130, 1–13.
Shunichi, T., Milward, S.E., Da-Yong, F., Wah Soon, C., Badger, M.R., 2009. How does cyclic electron flow alleviate photoinhibition in Arabidopsis? Plant Physiol. 149, 1560–1567.
Sterner, R.W., Elser, J.J., 2002. Ecological Stoichiometry: The Biology of Elements from Molecules to the Biosphere. Princeton University Press, Princeton, NJ, USA.

Van de Waal, D.B., Verspagen, J.M., Lurling, M., Van Donk, E., Visser, P.M., Huisman, J., 2009. The ecological stoichiometry of toxins produced by harmful cyanobacteria: an experimental test of the carbon-nutrient balance hypothesis. Ecol. Lett. 12, 1326–1335.

Van de Waal, D.B., Verspagen, J.M., Finke, J.F., Vournazou, V., Immers, A.K., Kardinaal, W.E., Tonk, L., Becker, S., Van Donk, E., Visser, P.M., Huisman, J., 2011. Reversal in competitive dominance of a toxic versus non-toxic cyanobacterium in response to rising CO_2. ISME J. 5, 1438–1450.

Verschoor, A.M., Van Dijk, M.A., Huisman, J.E.F., Van Donk, E., 2013. Elevated CO_2 concentrations affect the elemental stoichiometry and species composition of an experimental phytoplankton community. Freshw. Biol. 58, 597–611.

Verspagen, J.M., Van de Waal, D.B., Finke, J.F., Visser, P.M., Huisman, J., 2014a. Contrasting effects of rising CO_2 on primary production and ecological stoichiometry at different nutrient levels. Ecol. Lett. 17, 951–960.

Verspagen, J.M.H., Van, D.B., Waal, D., Finke, J.F., Visser, P.M., Donk, E.V., Huisman, J., 2014b. Rising CO_2 levels will intensify phytoplankton blooms in eutrophic and hypertrophic lakes. PLoS One 9, e104325.

Visser, P.M., Verspagen, J.M.H., Sandrini, G., Stal, L.J., Matthijs, H.C.P., Davis, T.W., Paerl, H.W., Huisman, J., 2016. How rising CO_2 and global warming may stimulate harmful cyanobacterial blooms. Harmful Algae 54, 145–159.

Vogt, R.J., St-Gelais, N.F., Bogard, M.J., Beisner, B.E., Del Giorgio, P.A., 2017. Surface water CO_2 concentration influences phytoplankton production but not community composition across boreal lakes. Ecol. Lett. 20, 1395–1404.

Wan, R., Chen, Y., Zheng, X., Su, Y., Li, M., 2016. Effect of CO_2 on microbial denitrification via inhibiting electron transport and consumption. Environ. Sci. Technol. 50, 9915–9922.

Wang, X., Hao, C., Zhang, F., Feng, C., Yang, Y., 2011. Inhibition of the growth of two blue-green algae species (*Microsystis aruginosa* and *Anabaena spiroides*) by acidification treatments using carbon dioxide. Bioresour. Technol. 102, 5742–5748.

Wang, S., Pan, X., Zhang, D., 2014. Effects of cadmium on the activities of photosystems of Chlorella pyrenoidosa and the protective role of cyclic electron flow. Chemosphere 107 (2), 480.

Wei, H., Shi-Bao, Z., Kun-Fang, C., 2010. Stimulation of cyclic electron flow during recovery after chilling-induced photoinhibition of PSII. Plant Cell Physiol. 51, 1922.

Wu, Y., Gao, K., Riebesell, U., 2010. CO_2-induced seawater acidification affects physiological performance of the marine diatom Phaeodactylum tricornutum. Biogeosciences 7, 2915–2923.

Xu, H., He, P., Wang, G., Shao, L., 2010. Three-dimensional excitation emission matrix fluorescence spectroscopy and gel-permeating chromatography to characterize extracellular polymeric substances in aerobic granulation. Water Sci. Technol. 61, 2931–2942.

Xu, H., Cai, H., Yu, G., Jiang, H., 2013a. Insights into extracellular polymeric substances of cyanobacterium *Microcystis aeruginosa* using fractionation procedure and parallel factor analysis. Water Res. 47, 2005–2014.

Xu, H., Yu, G., Jiang, H., 2013b. Investigation on extracellular polymeric substances from mucilaginous cyanobacterial blooms in eutrophic freshwater lakes. Chemosphere 93, 75–81.

Xu, H., Jiang, H., Yu, G., Yang, L., 2014. Towards understanding the role of extracellular polymeric substances in cyanobacterial *Microcystis aggregation* and mucilaginous bloom formation. Chemosphere 117, 815–822.

Yang, G., Gao, K., 2012. Physiological responses of the marine diatom Thalassiosira pseudonana to increased pCO_2 and seawater acidity. Mar. Environ. Res. 79, 142–151.

Yang, J., Tang, H., Zhang, X., Zhu, X., Huang, Y., Yang, Z., 2018. High temperature and pH favor Microcystis aeruginosa to outcompete Scenedesmus obliquus. Environ. Sci. Pollut. Res. Int. 25, 4794–4802.